Hindawi Publishing Corporation
Journal of Nanomaterials
Volume 2013, Article ID 790323, 9 pages
http://dx.doi.org/10.1155/2013/790323

Research Article

Optimal Size of Gold Nanoparticles for Surface-Enhanced Raman Spectroscopy under Different Conditions

Seongmin Hong and Xiao Li

Department of Chemistry, University of South Florida, Tampa, FL 33620, USA

Correspondence should be addressed to Xiao Li; xli@usf.edu

Received 29 November 2012; Accepted 13 May 2013

Academic Editor: Jun Li

Gold nanoparticles have been used as effective surface-enhanced Raman spectroscopy (SERS) substrates for decades. However, the origin of the enhancement and the effect of the size of nanoparticles still need clarification. Here, gold nanoparticles with different sizes from 17 to 80 nm were synthesized and characterized, and their SERS enhancement toward both 4-aminothiophenol and 4-nitrothiophenol was examined. For the same number of nanoparticles, the enhancement factor generated from the gold nanoparticles increases as the size of nanoparticles increases. Interestingly, when the concentration of gold or the total surface area of gold nanoparticles was kept the same, the optimal size of gold nanoparticles was found out to be around 50 nm when the enhancement factor reached a maximum. The same size effect was observed for both 4-aminothiophenol and 4-nitrothiophenol, which suggests that the conclusions drawn in this study might also be applicable to other adsorbates during SERS measurements.

1. Introduction

Surface-enhanced Raman spectroscopy (SERS) is a surface sensitive technique that provides high Raman scattering enhancement of molecules adsorbing on a rough metal surface, such as silver, gold, and copper [1, 2]. Presently, there are two well-accepted theories describing the mechanism of SERS amplification: electromagnetic enhancement and chemical enhancement. Electromagnetic enhancement (EME) is responsible for up to 10^6–10^7 increase of Raman scattering which occurs as the surface Plasmon gets excited by incident light and amplifies the electromagnetic field of the metal surface [1, 2]. Chemical enhancement, on the other hand, provides up to 10^2 increase of Raman scattering, and it happens when the molecule adsorbs strongly on the surface of the metal, which leads to changes of its polarizability. Due to the high enhancement, SERS technique has thus been studied extensively for the last few decades, and it provides many advantages including nondestructive nature, low detection limit, high sensitivity, and easy sample preparation. SERS has been widely applied in many different areas [3–10].

Metal nanoparticles (NPs) especially Ag and Au NPs have been widely employed in SERS because of their unique physical properties that depend on size and shape of the nanoparticles [11, 12]. Among the metals mentioned above, silver usually exhibits the highest SERS activity. It was reported that the optimal Ag nanoparticles size is 15 nm which generates the strongest SERS activity in solution [11]. Interestingly, the optimal size of Ag NPs was observed ca. 50 nm when off-resonance SERS is adopted [12]. On the other hand, gold has captured the most interests among recent studies. Gold metal is known to be biocompatible [10] and shows a strong excitation close to the IR region of light, which has attracted considerable interests in its use in biotechnological systems [13]. Various research groups have studied and reported the relationship between the enhancement and the shape and size of the immobilized gold NPs on a substrate using different analytes like 4-aminothiophenol (4-ATP) [14, 15] and 5,5′-dithiobis(2-nitrobenzioc acid) (DNBA) [16]. The results from all laboratories indicate that the SERS enhancement is highly dependent on many factors including the size of gold NPs, however, with controversial conclusions. When 4-ATP

adsorbed on immobilized gold NPs, the SERS intensity from gold NPs with the size of 30 nm was lower than that from gold NPs with the size of 18 nm [14, 15]. When 4-ATP was sandwiched between Au NPs and a smooth Au substrate, the SERS intensity was found out to increase as the size of the gold NPs increases [14, 15]. When labeled gold NPs were immobilized at a gold smooth surface, 60 nm NPs result in the largest SERS enhancement [16]. In addition, the SERS intensity from 4-mercaptobenzoic acid on gold nanoparticles was reported to increase as the size of the NPs increases in solution when the total number of nanoparticles was kept the same [17].

Therefore, in this study, we investigated and compared the SERS enhancement of gold NPs of different sizes using both 4-nitrothiophenol (4-NTP) and 4-aminothiophenol (4-ATP) as the target molecules to better compare our results with previous ones. The SERS intensities of target molecules were probed by adsorbing them onto gold nanoparticles of the average size of 17, 30, 40, 50, 60, and 80 nm created using further reduction method [18, 19]. SERS spectra were recorded by using 647 nm Argon-Krypton lasers on a confocal Raman microscope. Furthermore, we determined the SERS enhancement and size correlation of nanoparticles under three conditions including the same number of nanoparticles, the same total surface area of the nanoparticles, and the same concentration of gold in solution. Interestingly, different conclusions of the relationship were drawn under various conditions. The optimal size of gold NPs that provides the highest enhancement factor was found out while the concentration, and the total surface area and total number of the gold NPs were kept the same. This is the first time that the optimal size of gold NPs was established under various conditions in solution.

2. Experimental Methods

Hydrogen Tetrachloroaurate (III) trihydrate ($HAuCl_4 \cdot 3H_2O$, 99.9+%), trisodium citrate ($C_6H_5Na_3O_7 \cdot 2H_2O$, 99.9%), and Hydroxylamine Hydrochloride ($H_3NO \cdot HCl$, 99+%) were purchased from Fisher Scientific and were used as received. SERS tested sample, 4-nitrothiophenol (80%), and 4-aminothiophenol (97%) were purchased from Sigma-Aldrich and were used as received. All glassware was acid washed using sulfuric acid and nitric acid, and all of the solutions were prepared using deionized water (18.2 MΩ·cm) from a Cascada BIO and AN Lab Water System.

2.1. Synthesis of Gold Nanoparticles. Gold nanoparticles (NPs) of different sizes were synthesized by multiple reduction processes based on the work of Cyrankiewicz et al. [18] and Haiss et al. [19]. First, gold nanoparticles were synthesized by reduction of 0.5 mM $HAuCl_4$ with 1% trisodium citrate in aqueous solution [18]. After this step, gold NPs of the average size of 17 nm were obtained. Next, 2.50 mL of 25.4 mM $HAuCl_4$ and 3.00 mL of 0.20 M Hydroxylamine were added into the 17 nm gold seed solution to synthesize gold NPs with a larger size. After that step, gold NPs of the average size of 30 nm were obtained. Using 30 nm gold NPs as the seeds, various amounts of 25.4 mM $HAuCl_4$ and 0.20 M Hydroxylamine were added to the solution to synthesize larger gold NPs of different sizes [19]. In detail, 0.45 mL, 0.80 mL, and 1.3 mL $HAuCl_4$ and 0.70 mL, 1.5 mL, and 2.0 mL of Hydroxylamine were used to synthesize gold NPs with the average size of 40, 50, and 60 nm, respectively. To synthesize 80 nm gold NPs, 60 nm Au NPs were used as seed and 0.43 mL $HAuCl_4$ and 0.67 mL of Hydroxylamine were added. An extra amount of reducing agent was added to ensure complete reduction of gold. All of the solutions were dark red at the end. Colloidal solutions were kept in the dark during storage because of the photosensitivity concerns [20].

2.2. Sample Preparation. In order to create calibration plots for 4-ATP and 4-NTP, samples were prepared by first pipette mixing 1.00 mL of gold colloidal solutions with different amount of 4-ATP or 4-NTP; then for 4-NTP, 1.00 mL of 1 M NaCl was added into a glass cuvette. All of the measurements were done using exactly the same experimental conditions. Prepared samples were placed in the dark for 10 minutes before the measurement. This step helps to minimize the fluctuations of SERS spectra by allowing the colloidal solution to reach the equilibrium state.

2.3. UV-Vis, SEM, and SERS Measurements. UV-Vis absorption spectra of the colloidal solution were obtained with a Beckman Coulter DU 640 spectrometer. The UV-Vis spectra were used to elucidate the relative size of the particles in the solutions by comparing the location of the maximum peak wavelength in the spectra. Gold colloidal solutions were mixed with equal parts of deionized water and placed into quartz cuvette. The concentrations of gold colloidal solutions were adjusted to offset the UV-Vis spectrum for easy viewing. The concentrations were 0.083 mM, 0.040 mM, 0.015 mM, 0.017 mM, 0.019 mM, and 0.028 mM for gold NPs of the average size from 17 nm and 80 nm. The wavenumber range was set between 250 nm to 800 nm. The resolution of 0.5 nm was used to scan the gold colloidal solutions. UV-Vis spectra of the 17 nm to 80 nm gold colloidal solutions have been collected over a 4-week period of time to test the stability of the nanoparticles.

To measure the size of gold nanoparticles, Scanning Electron Microscopy (SEM) images were obtained using the Hitachi microscope (Hitachi S-800) located at the Nanotechnology Research and Education Center on the University of South Florida's Tampa Campus. Before the SEM measurements, the gold colloidal solutions were dropped (ca. 2 μL) on top of the silicon wafer and were air dried. The wafers were kept away from light because of the photosensitivity concerns. By imaging the particles using SEM [21], the size and shape of individual particles of gold were characterized as well as the size distribution of the particles.

All the SERS experiments were carried out using a Confocal Raman Microscopy (Olympus, IX71) purchased from Horiba Jovin Yvon, equipped with an Argon and Krypton laser (Coherent, Innova 70C series) producing 514 nm and 647 nm of wavelengths. For all experiments, an excitation laser with the wavelength at 647 nm has been applied with 40 mW of power, 3 s of exposure time, and 3 accumulations. The spectrum grating was 600, and the 20X microscopic

objective lens was used throughout the experiments. All of the results that were reported have been repeated independently for three times for the reproducibility. To examine the effect of nanoparticle size on the enhancement, either the concentration of gold, the total number, or the total surface area of the gold NPs was kept the same in the final sample solutions.

3. Results/Discussion

3.1. SEM Images of Different-Sized Au Nanoparticles. To measure the size and its distribution of gold NPs, SEM technique was applied to get image of the gold NPs. The size of gold NPs in each image was measured individually. At least 100 nanoparticles were counted for each sample to estimate the mean diameter and the relative standard deviation of the gold nanoparticles.

Figure 1 shows typical SEM images and the histograms of size distribution of gold nanoparticles with the mean diameter of 17, 30, 40, 50, 60, and 80 nm, respectively. The particle shape was nearly spherical for the nanoparticles of all sizes. The statistical analysis results of the Au nanoparticles including the mean size, standard deviation, and relative standard deviation are listed in Table 1. The standard deviation increases as the size of the gold NPs increases. However, the relative standard deviation values for the sizes around 40, 50, 60, and 80 nm of gold NPs are apparently lower than others. The size distribution of the gold nanoparticles is comparable to previous studies [17], which allow us to correlate the size of the nanoparticles with the SERS properties of the nanoparticles in solution.

3.2. UV-Vis Absorption Spectra of Gold Nanoparticles. Figure 2(a) shows the UV-Vis absorption spectra of gold nanoparticles of average size of 17, 30, 40, 50, 60, and 80 nm, respectively. The wavelength with maximum absorbance λ_{max} was found out to increase from 519 nm to 550 nm, as shown, in Table 1. As the size of Au NPs increases, the λ_{max} increases which agrees well with the previous conclusion that the maximum peak wavelength red-shifts as the relative particle size gets bigger [18, 22].

To test the stability of those gold nanoparticles, UV-Vis absorption spectra of 17 nm to 80 nm colloidal solutions were collected over a 4-week period of time. Figure 2(b) shows the change of the maximum absorbance of different gold colloidal solutions with time. Clearly, the absorption intensity of those gold colloidal solutions does not change much over a month, which indicates that gold NPs are stable within that time frame. This phenomenon is also approved by SERS measurements as the SERS activity of those gold nanoparticles changes little within the period of one month.

Once the average size and its distribution of gold NPs were determined using SEM and UV-Vis techniques, the concentration, number, and surface area of gold nanoparticles in the colloidal solutions with different sizes were calculated. Since more than enough reducing agent was added during synthesis, total reduction of gold is expected. Therefore, the number of gold NPs in the colloidal solution was estimated by (1) through dividing the total mass of gold in $HAuCl_4$ used to synthesize the gold NPs by the individual mass of a gold NP:

$$n = \frac{m_t}{m_i} = \frac{m_t}{DV} = \frac{m_t}{D4\pi r^3/3} = \frac{6m_t}{D\pi d^3}. \quad (1)$$

In (1), n is the number of nanoparticles; m_t is the total mass of Au in the solution; m_i is the mass of one nanoparticle; D is the density of Au assuming that the density does not change with the size of the nanoparticles; [23] r is the radius of the nanoparticle and d is the diameter of the nanoparticle.

Similarly, surface area of gold nanoparticles with certain size is calculated using (2) assuming that all nanoparticles are spherical:

$$A = \pi d^2 n = \frac{6\pi d^2 m_t}{D\pi d^3} = \frac{6m_t}{Dd}. \quad (2)$$

Table 1 shows the distribution of size, the calculated concentration, the number, and the surface area of the gold nanoparticles in different colloidal solutions when synthesized.

3.3. SERS Studies of 4-Aminothiophenol (4-ATP) to Test the Effect of Concentration, Number, and Surface Area of Nanoparticles on the Enhancement. SERS technique was applied to compare the enhancement of gold NPs with different sizes. Figure 3(a) shows the SERS spectra of 4-ATP collected with gold NPs with the size of 17, 30, 40, 50, 60, and 80 nm respectively. The observed peak positions of 4-ATP agree with the literature values [24, 25]. In detail, the peaks at 1079 and 1587 cm^{-1} are assigned to the stretching vibrations of C–S and C–C, respectively. Another peak at 390 cm^{-1} represents the bending vibration of C–S. The peak at 1079 cm^{-1}, as indicated by the arrow in Figure 3(a), was used to compare the intensity of the different gold solutions because it exhibits the highest intensity and is characteristic of 4-ATP [15]. The rest of the assignment of SERS peak of 4-ATP is summarized in Table 2.

Figures 4(a)–4(c) show the change of SERS analytical enhancement factor (AEF) of the vibration peak at 1079 cm^{-1} with the size of gold nanoparticles when (a) the number of gold NPs, (b) the total surface area of NPs, and (c) the concentration of gold were kept the same. The AEF shown in Figure 4 was calculated using (3), where I_{SERS} and I_{NR} are the intensity of the vibrational peak in SERS and normal Raman (NR) measurements, respectively, and C_{NR} and C_{SERS} are the concentration of 4-ATP or 4-NTP in NR measurements and the SERS measurements, respectively [26–28]:

$$EF = \frac{I_{SERS} C_{NR}}{I_{NR} C_{SERS}}. \quad (3)$$

Since SERS enhancement is mainly influenced by the surface adsorbed molecules, 0.18 μM, which was located in dynamic linear range of calibration plots of 4-ATP and 4-NTP, was used for the SERS measurements for more accurate analytical enhancement factor (AEF) measurement. The dynamic linear range of the analytes for the SERS measurements is determined using calibration plots for gold NPs with

Table 1: Size distribution, maximum peak wavelength in UV-Vis absorption spectra, and calculated concentration, number, and surface area of different gold colloidal solutions.

Size						
Mean (nm)	Standard deviation (nm)	Relative standard deviation (%)	λ_{max} (nm)	Concentration of gold (mM)	Number of gold NPs (/L)	Surface area of gold NPs (m^2/L)
17	5	29	510	0.25	$(2.1 \pm 0.9) \times 10^{16}$	19 ± 5
30	7	23	525	0.12	$(6 \pm 2) \times 10^{15}$	15 ± 3
40	6	15	530	0.045	$(8 \pm 2) \times 10^{14}$	4.1 ± 0.6
50	8	16	536	0.050	$(4 \pm 1) \times 10^{14}$	3.6 ± 0.6
60	8	13	540	0.056	$(3.1 \pm 0.6) \times 10^{14}$	3.5 ± 0.5
80	13	16	550	0.084	$(6 \pm 3) \times 10^{13}$	1.2 ± 0.4

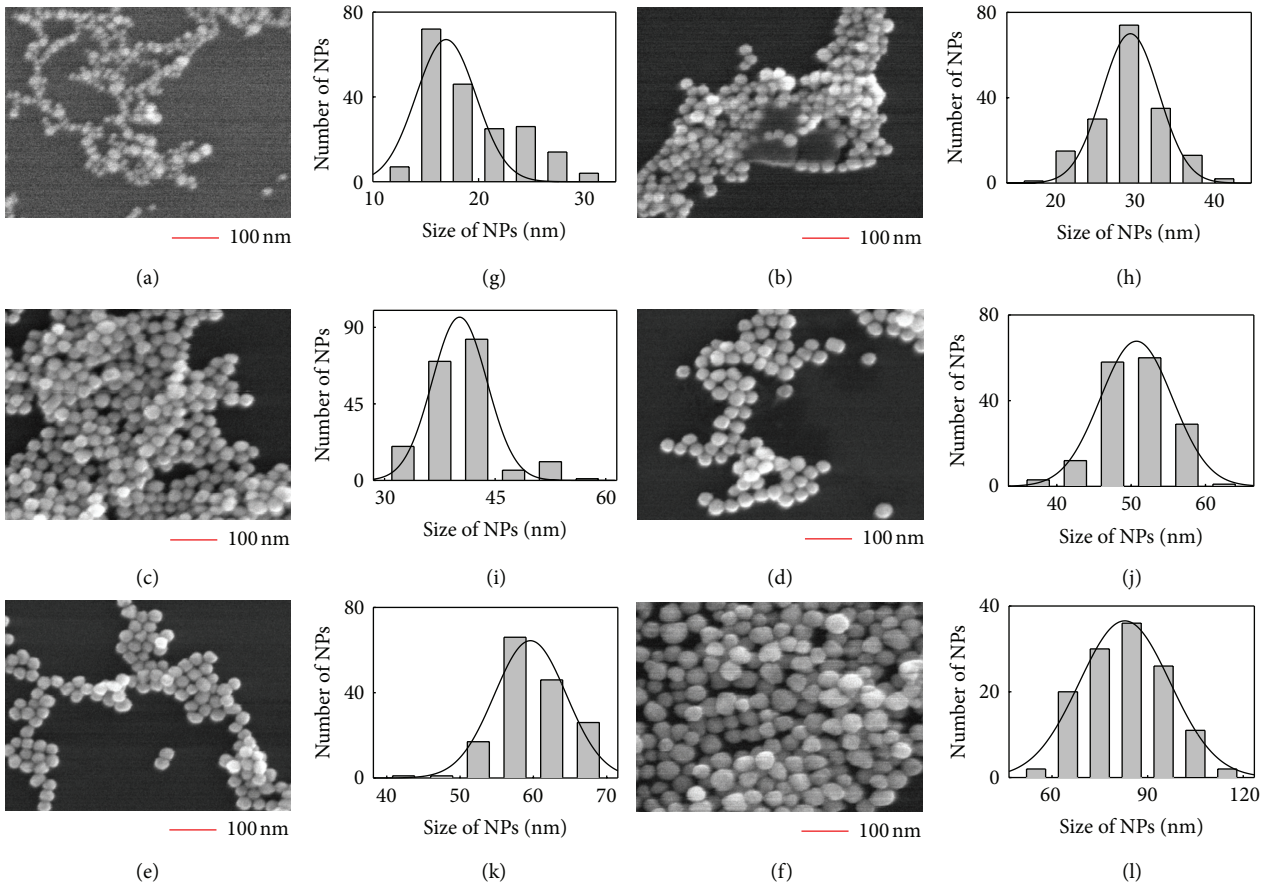

Figure 1: SEM images of the gold NPs with an average size of (a) 17 nm, (b) 30 nm, (c) 40 nm, (d) 50 nm, (e) 60 nm, and (f) 80 nm. The size histograms of the gold NPs with an average size of (g) 17 nm, (h) 30 nm, (i) 40 nm, (j) 50 nm, (k) 60 nm, and (l) 80 nm. The solid line in the size histograms is the simulation curve of Gaussian distribution.

different size. When the total numbers of gold NPs in the sample were kept the same, the SERS intensity increases as the size of the gold NPs increases, as shown in Figure 4(a). This observation can be easily understood due to the fact that as the size of the gold NPs increases, the surface area of the NPs increases; hence, the amount of 4-ATP molecules adsorbed on the surface increases, and so does the SERS intensity. Clearly, surface area of the SERS substrates is directly related to the enhancement achieved for a SERS measurement.

However, is the surface area the only reason for achieving high SERS enhancement? To answer this question, the spectra of 4-ATP from different colloidal solutions were collected by keeping the total surface area of the gold NPs the same. The results were shown in Figure 4(b). Interestingly, the highest enhancement was achieved from gold nanoparticles with a size ca. 50 nm. This result undoubtedly indicates that the SERS enhancement depends not only on the surface area of the SERS substrates but also on other factors such as the

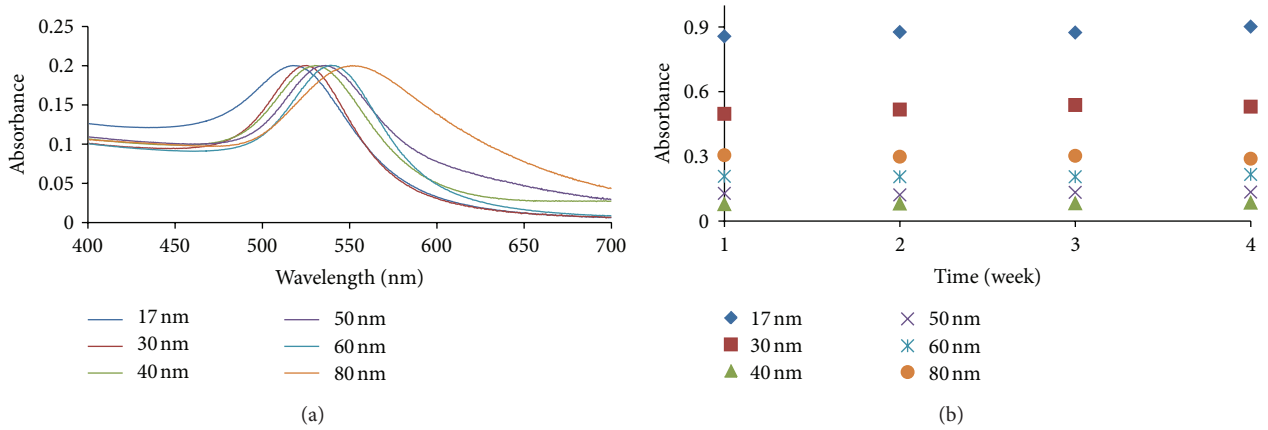

FIGURE 2: (a) The UV-Vis spectra of gold NPs of different size. The absorbance was normalized for better comparison. (b) The change of maximum absorbance of 17 to 80 nm gold NPs over 4 weeks. The concentrations were 0.083 mM for 17 nm, 0.040 mM for 30 nm, 0.015 mM for 40 nm, 0.017 mM for 50 nm, 0.019 mM for 60 nm, and 0.028 mM for 80 nm.

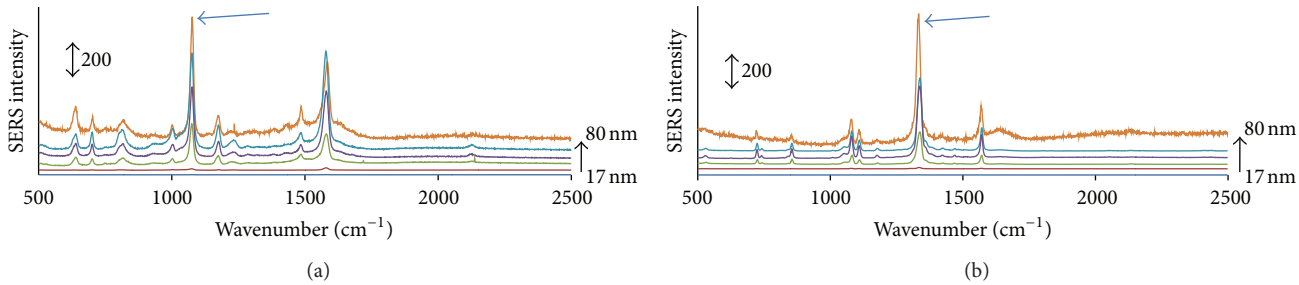

FIGURE 3: SERS spectra of (a) 0.25 μM 4-ATP and (b) 0.044 μM 4-NTP aqueous solution using gold nanoparticles with the size of 17, 30, 40, 50, 60, and 80 nm, respectively. The arrow of 4-ATP (1079 cm^{-1}) and 4-NTP (1340 cm^{-1}) indicates the peak used for the calculations of the enhancement factor.

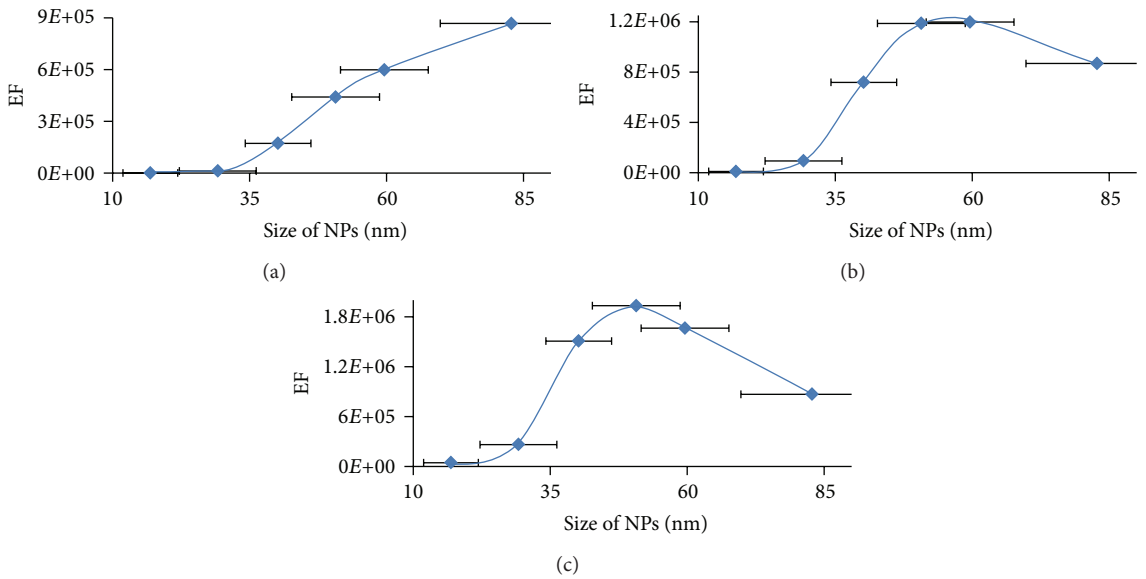

FIGURE 4: Experimental enhancement factor of 4-ATP, 1079 cm^{-1}, as a function of size of gold nanoparticles (a) when the number of gold NPs was kept the same, (b) when the surface area of all gold NPs was kept the same, and (c) when the concentration of gold was kept the same. The solid lines are just guiding of the eye. The error bar in x-axis is the standard deviation of the size of the nanoparticles while the error bar in y-axis is the standard deviation of enhancement factors from three experiments.

enhanced electromagnetic field generated from the surface plasma. It is known that the local electromagnetic enhancement increases with the increasing particle size [29]. But, as the nanoparticles size gets bigger, the convex shape, of the surface becomes flatter, the particles absorb less light and less inelastic scattering occurs on the surface, which leads to weakening of electromagnetic field on the surface and the overall SERS intensity [14, 30–32]. Moreover, previous study of the correlation between the surface plasmon resonance (SPR) properties of gold NPs and SERS spectra has revealed that the SP band red-shifts with increasing particles size. The largest SERS EF was found for the gold NPs with an SPR maximum between the wavelengths for laser excitation and for the vibrational band under study [16]. Therefore, as the size of the nanoparticles increases, the SPR moves close to the excitation wavelength of the laser (647 nm) and eventually away from that of the vibrational mode (696 nm). This explains our observations that the SERS EF generated from gold nanoparticles maximizes when the size of the gold NPs is around 50 nm. Interestingly, this conclusion agrees well with previous report when Au nanoparticles were immobilized on substrate [18].

Substrate enhancement factors (SEF) is another way of calculating enhancement factor, which is shown in (4), where I_{SERS} and I_{NR} are the intensities of the vibrational peak in SERS and normal Raman (NR) measurements, respectively, and N_{NR} and N_{SERS} are the total numbers of 4-ATP and 4-NTP in NR measurements and the surface concentration of the analyte in SERS measurements, respectively [26–28]:

$$\mathrm{EF} = \frac{I_{SERS} N_{NR}}{I_{NR} N_{SERS}}. \quad (4)$$

SEF considers the actual concentration of molecules and surface area of NP substrates that contribute to the SERS enhancement. This SEF can compromise the disadvantage of AEF where you have more than a monolayer of molecules present in sample. In this experiment, SEF was calculated for the size of gold NPs that showed highest AEF. For 4-ATP, the highest AEF was found with size around 50 nm of gold for both conditions where the concentration and surface area of gold were kept the same. The SEF for gold NPs with size around 50 nm was estimated to be 2.67×10^4.

Employing gold NPs in SERS experiment opened up more opportunities to study biological samples both in vivo and in vitro because of gold's biocompatibility. In addition, gold nanoparticles have attracted more and more attention as promising drug delivery means [10, 30]. To minimize possible toxicity effect of injecting gold NPs into the biological samples, the smallest possible amount of gold should be used for each measurement. Therefore, the effect of the gold NPs' size on their SERS enhancement was tested by keeping the concentration of the gold in the sample the same. The results were shown in Figure 4(c). The highest enhancement was achieved from gold nanoparticles with a size ca. 50 nm. According to the recent study by Chen and his colleagues, gold nanoparticles with the size bigger than 8 nm and smaller than 50 nm are toxic to the biological samples that they tested [33]. Therefore, using gold nanoparticle ca. 50 nm can not only minimize the possible toxic effect on biological samples but also maximize the SERS enhancement factor generated from the NPs.

3.4. SERS Studies of 4-Nitrothiophenol (4-NTP) to Test the Effect of Concentration, Number, and Surface Area of Nanoparticles on the Enhancement. To test whether the conclusions drawn above are specific to 4-ATP and also to compare our observations with previous reports, we performed the same study using 4-NTP as the target molecule. Figure 3(b) shows the SERS spectra of 4-NTP collecting from gold NPs with the size of 17, 30, 40, 50, 60, and 80 nm, respectively [24, 25]. The peaks at 1081, 1340, and 1587 cm^{-1} are due to the stretching vibrations of C–S, N–O, and C–C, respectively. The peak at 854 cm^{-1} represents the wagging vibration of C–H while the peak at 1110 cm^{-1} is assigned to the bending vibration of C–H. The peak at 1340 cm^{-1}, as indicated by the arrow in Figure 3(b), was used to compare the intensity of the different gold solution because it exhibits the highest intensity. The assignment of the SERS peaks of 4-NTP is summarized in Table 2.

Figures 5(a)–5(c) show the change of SERS AEF of the vibration peak at 1340 cm^{-1} with the size of gold nanoparticles when (a) the number of gold NPs, (b) the total surface area of NPs, and (c) the concentration of gold were kept the same. Generally, despite their similar chemical structure, big differences were observed between the SERS spectra and the EF of 4-NTP and those of 4-ATP even though the same experimental conditions including the SERS substrates were used. This was observed before and might be explained by the difference in their chemical structure between the nitro group of 4-NTP and the amine group of 4-ATP [24, 25]. As shown in Figure 5(a), when the number of gold nanoparticles was kept the same, the SERS EF increases as the size of the gold particle increases. Furthermore, Figures 5(b) and 5(c) show that the highest EF was achieved from gold nanoparticles around 50 nm when the surface area and the concentration of gold were kept the same, respectively. The SEF for 4-NTP for size 50 nm gold NPs were both 1.27×10^4 [26–28]. All of these results were nearly identical with those from 4-ATP. This clearly indicates that the conclusions drawn from 4-ATP and 4-NTP might also be applicable to other adsorbates when using Au nanoparticles as the SERS substrates for the detection.

4. Conclusions

Different sizes of gold nanoparticles were synthesized based on the work of Cyrankiewicz et al. [18] and Haiss et al. [19]. SEM technique was applied to determine the size and shape of the gold NPs. The average size of gold nanoparticles was found out to be 17, 30, 40, 50, 60, and 80 nm, respectively, with spherical shape. Gold NPs with the size of 50 nm exhibit the largest standard deviation. The red shift of λ_{max} value from UV-Vis absorption spectra of the colloidal solutions also indicates the size increment of gold NPs. Both the SERS activity and the UV-Vis absorption of gold NPs were observed to be stable for at least one month.

Table 2: SERS spectral peak assignment of 4-ATP[a] and 4-NTP[b].

SERS peak (cm^{-1}) of 4-ATP	Assignment	SERS peak (cm^{-1}) of 4-NTP	Assignment
390	δ (CS)	332	δ (CS)
635	γ (CCC)	723	π (CH) + π (CS) + π (CC)
1005	γ (CC) + γ (CCC)	854	π (CH)
1079	ν (CS)	1081	ν (CS)
1177	ν (CH)	1110	δ (CH)
1485	ν (CC) + δ (CH)	1340	ν (NO_2)
1587	ν (CC)	1569	ν (CC)

[a]The peak assignment of 4-ATP is from [24, 25].
[b]The peak assignment of 4-NTP is from [25].

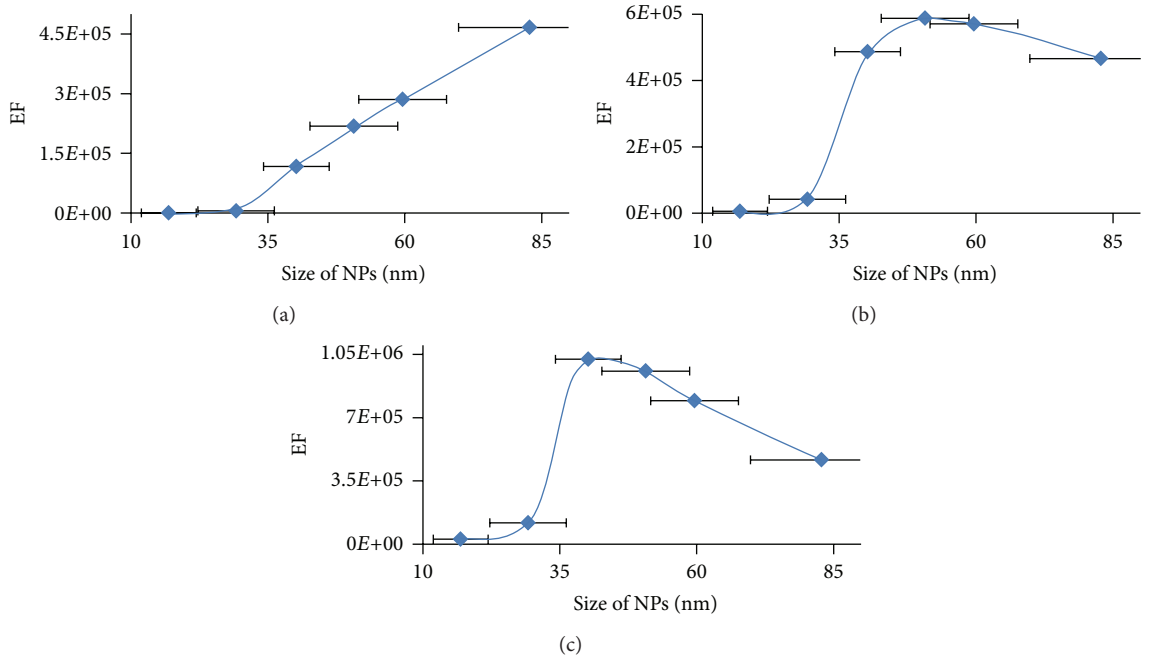

Figure 5: Experimental enhancement factor of 4-NTP, calculated from peak at 1340 cm^{-1}, as a function of size of gold nanoparticles (a) when the number of gold NPs was kept the same, (b) when the surface area of all gold NPs was kept the same, and (c) when the concentration of gold was kept the same. The solid lines are just guiding of the eye. The error bar in x-axis is the standard deviation of the size of the nanoparticles while the error bar in y-axis is the standard deviation of enhancement factors from three experiments.

Using gold NPs with different sizes, the SERS spectra of 4-ATP and 4-NTP were collected. In order to find out the optimal size of the gold NPs that provides the highest enhancement factor, either the concentration of gold, the number, or the surface area of the gold NPs was kept the same. When the number of gold NPs was kept constantly, there was a positive linear relationship between the size of the NPs and the EF based on the SERS measurements. This phenomenon can be explained by the fact that surface area increases as the size of the gold NPs increases when the total number of NPs is the same, which leads to the higher SERS intensity. However, interesting phenomena were observed when keeping the total surface area of gold NPs or the concentration of gold constant. As shown in Figures 4(b), 4(c), 5(b), and 5(c), the highest intensity was observed when the size of gold NPs was around 50 nm when either the surface area of gold NPs or the concentration of gold was the same. Such phenomena might be explained by the relationship between the SERS enhancement and the size or the surface area of the NPs.

More importantly, the same correlations were obtained for both 4-ATP and 4-NTP. This indicates that such conclusions might not be highly sensitive to the chemical structure of the target molecules. Instead, the conclusions might also be applicable to other adsorbates. Generally, gold NPs of the size around 50 nm are optimal when the surface area or the concentration is critical. In addition, gold NPs with size around 50 nm show minimum toxicity effect on biological samples. This conclusion is essential when SERS is used to detect important biomolecules in biological samples so that minimum amount of gold can be introduced into the biological system to achieve lowest toxicity possible while the highest SERS sensitivity can be reached at the same time.

Acknowledgments

This research was supported by James & Esther King Biomedical Research Program, Florida Department of Health, and the University of South Florida starting fund. The authors thank Professor Wonkuk Kim from the Department of Mathematics and Statistics for his expertise in statistics.

References

[1] L. Xia, J. Wang, S. Tong, G. Liu, J. Li, and H. Zhang, "Design and construction of a sensitive silver substrate for surface-enhanced Raman scattering spectroscopy," *Vibrational Spectroscopy*, vol. 47, no. 2, pp. 124–128, 2008.

[2] Y. Wang, H. Wei, B. Li et al., "SERS opens a new way in aptasensor for protein recognition with high sensitivity and selectivity," *Chemical Communications*, no. 48, pp. 5220–5222, 2007.

[3] S. Nie and S. R. Emory, "Probing single molecules and single nanoparticles by surface-enhanced Raman scattering," *Science*, vol. 275, no. 5303, pp. 1102–1106, 1997.

[4] R. J. Dijkstra, W. J. J. M. Scheenen, N. Dam, E. W. Roubos, and J. J. ter Meulen, "Monitoring neurotransmitter release using surface-enhanced Raman spectroscopy," *Journal of Neuroscience Methods*, vol. 159, no. 1, pp. 43–50, 2007.

[5] J. Ni, R. J. Lipert, G. B. Dawson, and M. D. Porter, "Immunoassay readout method using extrinsic raman labels adsorbed on immunogold colloids," *Analytical Chemistry*, vol. 71, no. 21, pp. 4903–4908, 1999.

[6] M. Moskovits, "Spectroscopy: expanding versatility," *Nature*, vol. 464, no. 7287, p. 357, 2010.

[7] R. A. Alvarez-Puebla and L. M. Liz-Marzán, "SERS-based diagnosis and biodetection," *Small*, vol. 6, no. 5, pp. 604–610, 2010.

[8] I. Mannelli and M. P. Marco, "Recent advances in analytical and bioanalysis applications of noble metal nanorods," *Analytical and Bioanalytical Chemistry*, vol. 398, no. 6, pp. 2451–2469, 2010.

[9] T. Vo-Dinh, H. N. Wang, and J. Scaffidi, "Plasmonic nanoprobes for SERS biosensing and bioimaging," *Journal of Biophotonics*, vol. 3, no. 1-2, pp. 89–102, 2010.

[10] J. Kneipp, H. Kneipp, B. Wittig, and K. Kneipp, "Novel optical nanosensors for probing and imaging live cells," *Nanomedicine*, vol. 6, no. 2, pp. 214–226, 2010.

[11] C. S. Seney, B. M. Gutzman, and R. H. Goddard, "Correlation of size and surface-enhanced raman scattering activity of optical and spectroscopic properties for silver nanoparticles," *Journal of Physical Chemistry C*, vol. 113, no. 1, pp. 74–80, 2009.

[12] K. G. Stamplecoskie, J. C. Scaiano, V. S. Tiwari, and H. Anis, "Optimal size of silver nanoparticles for surface-enhanced raman spectroscopy," *Journal of Physical Chemistry C*, vol. 115, no. 5, pp. 1403–1409, 2011.

[13] P. K. Jain, X. Huang, I. H. El-Sayed, and M. A. El-Sayed, "Review of some interesting surface plasmon resonance-enhanced properties of noble metal nanoparticles and their applications to biosystems," *Plasmonics*, vol. 2, no. 3, pp. 107–118, 2007.

[14] S. C. Boca, C. Farcau, and S. Astilean, "The study of Raman enhancement efficiency as function of nanoparticle size and shape," *Nuclear Instruments and Methods in Physics Research Section B*, vol. 267, no. 2, pp. 406–410, 2009.

[15] J. K. Yoon, K. Kim, and K. S. Shin, "Raman scattering of 4-aminobenzenethiol sandwiched between Au nanoparticles and a macroscopically smooth Au substrate: effect of size of Au nanoparticles," *Journal of Physical Chemistry C*, vol. 113, no. 5, pp. 1769–1774, 2009.

[16] J. D. Driskell, R. J. Lipert, and M. D. Porter, "Labeled gold nanoparticles immobilized at smooth metallic substrates: systematic investigation of surface plasmon resonance and surface-enhanced raman scattering," *Journal of Physical Chemistry B*, vol. 110, no. 35, pp. 17444–17451, 2006.

[17] P. N. Njoki, I. I. S. Lim, D. Mott et al., "Size correlation of optical and spectroscopic properties for gold nanoparticles," *Journal of Physical Chemistry C*, vol. 111, no. 40, pp. 14664–14669, 2007.

[18] M. Cyrankiewicz, T. Wybranowski, and S. Kruszewski, "Study of SERS efficiency of metallic colloidal systems," *Journal of Physics: Conference Series*, vol. 79, no. 1, Article ID 012013, 2007.

[19] W. Haiss, N. T. K. Thanh, J. Aveyard, and D. G. Fernig, "Determination of size and concentration of gold nanoparticles from UV-Vis spectra," *Analytical Chemistry*, vol. 79, no. 11, pp. 4215–4221, 2007.

[20] E. Y. Hleb and D. O. Lapotko, "Photothermal properties of gold nanoparticles under exposure to high optical energies," *Nanotechnology*, vol. 19, no. 35, Article ID 355702, 2008.

[21] J. E. Herrera and N. Sakulchaicharoen, "Microscopic and spectroscopic characterization of nanoparticles," *Drugs and the Pharmaceutical Sciences*, vol. 191, p. 239, 2009.

[22] J. A. Creighton, "Metal colloids," in *Surface Enhanced Raman Scattering*, R. K. Chang and T. E. Furtak, Eds., p. 315, Plenum, New York, NY, USA, 1982.

[23] Z. Kolska, J. Riha, V. Hnatowicz, and V. Svorcik, "Lattice parameter and expected density of Au nano-structures sputtered on glass," *Materials Letters*, vol. 64, no. 10, pp. 1160–1162, 2010.

[24] K. Kim and H. S. Lee, "Effect of Ag and Au nanoparticles on the SERS of 4-aminobenzenethiol assembled on powdered copper," *Journal of Physical Chemistry B*, vol. 109, no. 40, pp. 18929–18934, 2005.

[25] M. E. Abdelsalam, "Surface enhanced raman scattering of aromatic thiols adsorbed on nanostructured gold surfaces," *Central European Journal of Chemistry*, vol. 7, no. 3, pp. 446–453, 2009.

[26] V. S. Tiwari, T. Oleg, G. K. Darbha, W. Hardy, J. P. Singh, and P. C. Ray, "Non-resonance SERS effects of silver colloids with different shapes," *Chemical Physics Letters*, vol. 446, no. 1–3, pp. 77–82, 2007.

[27] E. C. Le Ru, E. Blackie, M. Meyer, and P. G. Etchegoin, "Surface enhanced Raman scattering enhancement factors: a comprehensive study," *Journal of Physical Chemistry C*, vol. 111, no. 37, pp. 13794–13803, 2007.

[28] W. B. Cai, B. Ren, X. Q. Li et al., "Investigation of surface-enhanced Raman scattering from platinum electrodes using a confocal Raman microscope: dependence of surface roughening pretreatment," *Surface Science*, vol. 406, no. 1–3, pp. 9–22, 1998.

[29] K. L. Kelly, E. Coronado, L. L. Zhao, and G. C. Schatz, "The optical properties of metal nanoparticles: the influence of size, shape, and dielectric environment," *Journal of Physical Chemistry B*, vol. 107, no. 3, pp. 668–677, 2003.

[30] S. Ghoshal, D. Mitra, S. Roy, and D. D. Majumder, "Biosensors and biochips for nanomedical applications: a review," *Sensors and Transducers Journal*, vol. 113, no. 2, pp. 1–17, 2010.

[31] S. A. Maie, *Plasmonics: Fundamentals and Applications*, Springer, New York, NY, USA, 1st edition, 2006.

[32] M. Moskovits, "Surface-enhanced spectroscopy," *Reviews of Modern Physics*, vol. 57, no. 3, pp. 783–826, 1985.

[33] Y. S. Chen, Y. C. Hung, I. Liau, and G. S. Huang, "Assessment of the in vivo toxicity of gold nanoparticles," *Nanoscale Research Letters*, vol. 4, no. 8, pp. 858–864, 2009.